



Contents lists available at ScienceDirect



# Catalysis Today

journal homepage: [www.elsevier.com/locate/cattod](http://www.elsevier.com/locate/cattod)

## Effects of co-feeding with nitrogen-containing compounds on the performance of supported cobalt and iron catalysts in Fischer–Tropsch synthesis

Vitaly V. Ordovsky<sup>a</sup>, Alexandre Carvalho<sup>a,b</sup>, Benoit Legras<sup>a</sup>, Sébastien Paul<sup>a</sup>, Mirella Virginie<sup>a</sup>, Vitaly L. Sushkevich<sup>c</sup>, Andrei Y. Khodakov<sup>a,\*</sup>

<sup>a</sup> Unité de Catalyse et de Chimie du Solide—UMR CNRS 8181, Université Lille, Ecole Centrale de Lille, 59655 Villeneuve d'Ascq Cedex, France

<sup>b</sup> Department of Chemical Engineering, Federal University of Rio Grande do Sul, Porto Alegre, RS 90040-040, Brazil

<sup>c</sup> Department of Chemistry, Lomonosov Moscow State University, 119991, Leninsky Gory 1, Moscow, Russia

### ARTICLE INFO

#### Article history:

Received 12 October 2015

Received in revised form

14 December 2015

Accepted 17 December 2015

Available online xxx

#### Keywords:

Biosyngas

Fischer–Tropsch

Catalyst

Cobalt

Iron

Nitrides

Nitrogen impurities

Acetonitrile

### ABSTRACT

The performance of supported cobalt and iron catalysts in low and high temperature Fischer–Tropsch synthesis was investigated in the presence of small amounts of ammonia in syngas. Ammonia was co-fed to the reactor either by in-situ hydrolysis of acetonitrile or by addition of aqueous ammonia.

The addition of acetonitrile and ammonia resulted in significant irreversible deactivation of alumina supported cobalt catalysts. Lower methane and higher C<sub>5+</sub> hydrocarbon selectivities were observed. Iron based catalysts did not show any noticeable deactivation in the presence of acetonitrile or ammonia. Moreover, Fischer–Tropsch reaction rate slightly increased after addition of the nitrogen-containing compounds to silica and alumina supported samples. Lower methane selectivity and higher C<sub>2</sub>–C<sub>4</sub> olefin to paraffin ratio were observed in the presence of ammonia when the catalysts were reduced in hydrogen. Iron catalysts activated in carbon monoxide did not demonstrate any significant effect of ammonia on the selectivity. The catalytic data were explained by irreversible formation of inactive cobalt nitrides in cobalt catalysts and transformation of metallic iron and iron oxides in the presence of acetonitrile and ammonia into iron nitrides and iron carbides active in Fischer–Tropsch synthesis.

© 2015 Elsevier B.V. All rights reserved.

## 1. Introduction

The Fischer–Tropsch (FT) technology converts syngas produced from coal, natural gas, shell gas and biomass into hydrocarbons and oxygenates which can be further upgraded to fine chemicals and fuels. Both cobalt and iron catalysts are used for FT synthesis on the industrial scale. Cobalt catalysts are the catalysts of choice for low temperature FT synthesis, which produces middle distillates and waxes [1,2], while iron catalysts are mostly used in high temperature FT synthesis [3] which manufactures both fuels and petrochemicals. Catalyst deactivation is a major challenge for both cobalt and iron based FT catalysts [4,5]. The mechanism for catalyst deactivation in FT synthesis often includes a combination of different phenomena: poisoning, surface carbon formation, sintering, carbidization (for cobalt catalysts), oxidation, surface reconstruction, attrition... FT catalysts are particularly sensitive

to the presence of impurities in the reaction feed. Thus, purification of the syngas is an important and often very expensive part of the whole technology.

Continuous depletion to fossil resources and strategy for diversification of energy supplies have led to continuously growing interest in the development of new technologies such as BTL (Biomass-to-Liquids) which aim at producing hydrocarbons and oxygenates from renewable resources (e.g. lignocellulosic biomass and organic waste). The biosyngas can be produced from biomass using gasification. The presence of various impurities and poisons specific of biosyngas and gasification process such as tar, particulates, ammonia, hydrochloric acid and sulphur gases [6] can strongly affect the performance of cobalt and iron FT catalysts. The particularities of FT synthesis with biosyngas have been discussed in several reviews [6–9].

Among these impurities, sulphur compounds may cause irreversible deactivation of FT catalysts. A number of reports [10–17] have recently addressed the effect of sulphur impurities on the stability of iron and cobalt FT catalysts. Much less attention has been paid so far to the effects of nitrogen compounds in syngas on the

\* Corresponding author. Fax: +33 3 20 43 65 61.

E-mail address: [andrei.khodakov@univ-lille1.fr](mailto:andrei.khodakov@univ-lille1.fr) (A.Y. Khodakov).

performance and stability of FT catalysts. The effect of ammonia [18,19] on the catalytic performance has been shown to be different for cobalt and iron FT catalysts. The reported results however, have been rather contradictory. Borg et al. [15] studied the catalytic performance of alumina and titania supported catalysts in the presence of 4 ppm of NH<sub>3</sub> in syngas. No effect of ammonia on the catalytic performance was observed. LeVennes et al. [20] found that nitrogen compounds produce reversible effect on the catalytic performance of cobalt catalysts. The catalyst activity was restored by treatment in pure hydrogen. Pendyala et al. [21] studied the effect of addition of ammonia on the performance of platinum promoted cobalt/alumina catalysts. A significant irreversible catalyst deactivation was observed at ammonia levels from 1 to 1200 ppmw. In addition, in the presence of ammonia, the catalyst exhibited lower methane and higher C<sub>5+</sub> hydrocarbon selectivity which were attributed to selective poisoning of the methanation sites. Ma et al. [22] studied the effect of different ammonia containing compounds on the performance of precipitated iron catalysts in a slurry reactor. No deactivation was observed at low ammonia concentrations, while important catalyst deactivation was observed at concentrations of ammonia higher than 400 ppm. In the work of Sango et al. [23] significant amounts of ammonia (up to 10 wt.%) were added to the syngas feed over unsupported iron catalysts. The catalysts did not show any noticeable deactivation at the ammonia concentration below 2% wt. In addition to the usual FT products such as hydrocarbons and oxygenates, the reaction yielded long chained aliphatic amines, nitriles and amides, while the selectivities to alcohols, aldehydes and organic acids were much lower in the presence of ammonia.

The present report addresses the impact of addition of small amounts of acetonitrile and ammonia (1500 and 2500 ppmv) to the syngas feed on the catalytic performance of supported iron and cobalt catalysts. In particular, the effects of co-fed acetonitrile and ammonia on CO conversion, methane, light olefins, C<sub>5+</sub> hydrocarbon selectivities, catalyst stability and catalyst structure are discussed in this work. The catalytic performance has been evaluated in a Florence high-throughput system [24] (Avantium®) equipped with 16 parallel fixed-bed milli-reactors under typical conditions of low and high temperature FT syntheses.

## 2. Experimental

### 2.1. Catalyst preparation

Commercial γ-alumina containing 5% of silica (Al<sub>2</sub>O<sub>3</sub>, Siralox SASOL) was used as support for preparation of cobalt catalysts. The catalysts were prepared by incipient wetness impregnation with aqueous solutions of cobalt nitrate. The concentrations of the impregnation solutions were calculated to obtain 15 wt.% cobalt in the final catalysts. The alumina supported catalyst containing 25 wt.% Co was prepared using the two-step impregnation. In case of Pt-promoted samples, an additional incipient wetness impregnation of Co/γ-Al<sub>2</sub>O<sub>3</sub> with aqueous solutions of hydrogen hexachloroplatinate (H<sub>2</sub>PtCl<sub>6</sub>), (Sigma-Aldrich) was carried out. The platinum content was 0.1 wt.% in the final catalysts. After impregnation and drying the cobalt catalysts were calcined in air flow at 400 °C for 6 h with a 1 °C/min temperature ramping.

Iron catalysts were prepared using commercial amorphous silica (SiO<sub>2</sub>, CARIAC T Q-10, Fuji Silysia), alumina (Siralox, Sasol), activated carbon and carbon nanotubes. Activated carbon (AC) was provided by CEKA S.A., washed and then heated with 1 M solution of nitric acid at 50 °C for 2 h. Multi-wall carbon nanotubes (CNT, purity ≥95%, outer diameter 20–30 nm) were purchased from the Chengdu Limited Company of Organic Chemistry (CCOC) in China. They were prepared by chemical vapour deposition. The raw CNTs

were refluxed for 16 h in concentrated HNO<sub>3</sub> (65 wt.%) at 120 °C in an oil bath. Then, the mixture was filtered and thoroughly washed with distilled water until the neutral pH was reached. The washed carbon nanotubes were then dried overnight at 100 °C.

The iron catalysts were prepared by incipient wetness impregnation of the relevant supports with aqueous solutions of hydrous iron nitrate (Fe(NO<sub>3</sub>)<sub>3</sub>·9H<sub>2</sub>O). The concentrations of the impregnating solutions were calculated to obtain 10 wt.% iron in the final catalysts. After impregnation the catalysts were dried overnight in an oven at 100 °C. Then the catalysts supported by silica and alumina were calcined in a flow of air, while the carbon supported samples were calcined in nitrogen flow at 400 °C for 6 h with a 1 °C/min temperature ramping.

The catalysts are labelled as Mx%/Support, where x indicates metal content in the catalyst, M stands for metal (Co or Fe) and Support specifies the support used (Al<sub>2</sub>O<sub>3</sub>, SiO<sub>2</sub>, AC or CNT). The platinum content is indicated in the Pt-promoted catalysts.

### 2.2. Characterization techniques

The BET surface area, pore volume and average pore diameter were determined by N<sub>2</sub> physisorption using a Micromeritics ASAP 2000 automated system. The samples were degassed under vacuum at <10 μm Hg in the Micromeritics ASAP 2000 at 300 °C for 4 h prior to N<sub>2</sub> physisorption.

The ex situ X-ray powder diffraction (XRD) measurements were conducted using a Bruker AXS D8 diffractometer using Cu(Kα) radiation ( $\lambda = 0.1538 \text{ nm}$ ). The XRD patterns were collected in 20–70° (2θ) range. The identification was carried out by comparison with JCPDF standard spectra software. The average crystallite size of Fe<sub>3</sub>O<sub>4</sub>, Fe<sub>2</sub>O<sub>3</sub> and Co<sub>3</sub>O<sub>4</sub> was calculated using the diffraction lines according to Scherrer's equation [25].

The FTIR spectra were recorded with a Nicolet Protégé 460 FT-IR spectrometer at 4 cm<sup>-1</sup> optical resolution. Due to high cobalt content, all catalysts were diluted with α-Al<sub>2</sub>O<sub>3</sub> (1:1). Prior to the measurements, 20 mg of sample was pressed in self-supporting discs and activated in the IR cell attached to a vacuum line at 400 °C for 4 h followed by reduction in hydrogen at 400 °C. After the reduction, water formed was evacuated at 400 °C for 1 h. Dose per dose adsorption of CO was carried out in the low-temperature cell in liquid nitrogen. In several experiments, the catalysts were pre-treated *in situ* with NH<sub>3</sub> at 280 °C. Spectra processing was performed by OMNIC 7.3 software.

The cobalt catalysts after catalytic tests in a Florence high throughput unit conducted in the presence of acetonitrile were characterized by temperature-programmed desorption (TPD). The samples were weighed (50 mg) and loaded in the middle of a quartz tube. Both ends of the quartz tube were sandwiched with quartz wool. The signals were recorded by a mass spectrometer.

The SSITKA apparatus used in this work is described in Ref. [26]. It contains two independent feed lines. The first line is dedicated to unlabeled compounds and tracer (CO, H<sub>2</sub>, He and Ne), the second one to the isotopic compounds (<sup>13</sup>CO). The pressure transducers are used to adjust the same pressure drop for both lines. Isotopic switches were realized using a two-position four ways Valco-valve and monitored with QMG 432 Omnistar in the Faraday mode. In the first experiment, the Co25%0.1%Pt/Al<sub>2</sub>O<sub>3</sub> catalyst was reduced hydrogen at 400 °C for 3 h and then exposed to syngas (H<sub>2</sub>/CO = 5) at atmospheric pressure at 220 °C. After conducting 13 h of the reaction in the syngas, the periodic switches were performed from <sup>12</sup>CO/H<sub>2</sub>/He/Ne to <sup>13</sup>CO/H<sub>2</sub>/He with simultaneous measurement of the isotopic transient responses. In the second experiment, the catalyst after reduction in hydrogen was exposed to the flow of gaseous NH<sub>3</sub> at 220 °C and atmospheric pressure for 2 h. Then the ammonia flow was stopped and the syngas with H<sub>2</sub>/CO = 5 was directed to the catalyst. After conducting 13 h of the FT reaction in

**Table 1**

Supports used for preparation of cobalt and iron catalysts.

Catalyst	N <sub>2</sub> adsorption over supports		
	S <sub>BET</sub> , (m <sup>2</sup> /g)	V <sub>tot</sub> , (cm <sup>3</sup> /g)	Pore size, (nm)
Al <sub>2</sub> O <sub>3</sub>	175	0.45	8.3
CNT	163	0.56	5
SiO <sub>2</sub>	307	1.31	17.5
AC	558	0.4	—

syngas at atmospheric pressure, the switches from <sup>12</sup>CO/H<sub>2</sub>/He/Ne to <sup>13</sup>CO/H<sub>2</sub>/He were performed on the catalyst pre-treated with NH<sub>3</sub>.

### 2.3. Catalytic tests

Carbon monoxide hydrogenation was carried out in a Florence high throughput unit (Avantium®) [24], equipped with 16 parallel milli-fixed reactors ( $d = 2$  mm) operating at total pressure of 20 bar, H<sub>2</sub>/CO = 2 molar ratio and GHSV = 3000–16 000 cm<sup>3</sup> g<sub>cat</sub><sup>-1</sup> h<sup>-1</sup>. Prior to the catalytic tests, all the samples were activated in a flow of H<sub>2</sub> at atmospheric pressure during 10 h at 400 °C. For comparison, several Fe based catalysts have been also activated in CO at 350 °C. During the reduction, the temperature ramp was 3 °C/min. After the reduction, the catalysts were cooled down to 180 °C and a flow of premixed syngas was gradually introduced through the catalysts. When pressure attained 20 bar, the temperature was slowly increased to 220 °C and 300 °C for cobalt and iron catalysts, respectively. The gaseous reaction products were analysed by on-line gas chromatography. Analysis of permanent gases was performed using a Molecular Sieve column and a thermal conductivity detector. Carbon dioxide and C<sub>1</sub>–C<sub>4</sub> hydrocarbons were separated in a PPQ column and analysed by a thermoconductivity detector. C<sub>5</sub>–C<sub>12</sub> hydrocarbons were analysed using CP-Sil5 column and a flame-ionization detector. High-molecular-weight products were collected at atmospheric pressure in the vials heated at 80 °C. The carbon monoxide contained 5% of helium, which was used as an internal standard for calculating carbon monoxide conversion. The reaction rates expressed in mol g<sub>cat</sub><sup>-1</sup> s<sup>-1</sup>, were defined as the number of moles of CO converted per second per gram of catalyst. The product selectivity (S) was reported as the percentage of CO converted into a given product and is expressed on carbon basis.

The reaction runs with pure syngas were conducted for the first 24 h on stream. Then acetonitrile was introduced to the syngas feed. Small amounts of acetonitrile or aqueous ammonia were added using a HPLC pump with liquid flow rates of 5 and 10 µL/min to get respectively 1500 and 2500 ppmv in the gas feed. First, 1500 ppmv was maintained for 12 h. Then, addition was adjusted to 2500 ppmv for 12 h and finally stopped for 24 h. The catalyst was then again exposed to three times to 2500 ppm of CH<sub>3</sub>CN for 12 h separated by the periods of 12 h when it was exposed to the pure gas. The experimental procedure for acetonitrile and ammonia addition is displayed in Fig. 1.

## 3. Results and discussion

### 3.1. Catalyst characterisation

The BET surface area, total pore volume and pore diameter of the supports used for synthesis of cobalt and iron catalysts are shown in Table 1. The textural properties of Siralox are typical for γ-alumina with the BET surface area of 170 m<sup>2</sup>/g and pore sizes of about 8 nm. Large mesopores formed by volume between globules were detected in the commercial CARIACT Q-10 silica with the surface area of 300 m<sup>2</sup>/g. A relatively large surface area (557 m<sup>2</sup>/g) and micropores were observed in the activated carbon. The nanotubes

of the acid-treated CNT have uniform diameters of about 5 nm. Relatively high surface area of these materials suggests the presence of open caps.

The crystallite size of cobalt and iron oxides in the calcined supported catalysts was evaluated from XRD patterns using Scherrer's equation. Co<sub>3</sub>O<sub>4</sub> was the only cobalt phase detected by XRD in the alumina supported catalysts. In agreement with previous reports [27,28], the cobalt crystallite size was about 10–13 nm and was not much affected by cobalt content. Hematite (Fe<sub>2</sub>O<sub>3</sub>) was the main iron phase in silica iron supported catalysts with the crystallite size of 17.5 nm. Very broad XRD patterns relevant to iron oxides were detected in the alumina supported catalysts. This suggests the presence of very small particles of iron oxide (<5 nm) and high iron dispersion on the alumina support.

Magnetite (Fe<sub>3</sub>O<sub>4</sub>) was the major iron phase identified in the iron catalysts supported on carbon supports which were calcined in nitrogen. Larger magnetite crystallites were observed in carbon nanotubes ( $d_{Fe_3O_4} = 12.3$  nm) compared to activated carbon ( $d_{Fe_3O_4} = 6.7$  nm). Further information about the structure of supported cobalt and iron catalysts used in this work is available from previous publications [29–34].

### 3.2. FT synthesis with pure syngas

The catalytic performance data of cobalt and iron catalysts in FT synthesis measured respectively at 220 °C and 300 °C in pure syngas are shown in Table 2. Methane, light olefins, light paraffins, C<sub>5+</sub> hydrocarbons and water are the main reaction products on cobalt catalysts under these conditions. Only very small amounts of carbon dioxide can be detected. The FT reaction rate on cobalt catalysts principally depends on cobalt content in the catalysts and platinum promotion. Platinum promotion results almost in a two times increase in the reaction rate. In agreement with previous reports [35–37], higher FT reaction rate on Pt promoted cobalt catalysts was principally attributed to better cobalt reducibility. For the platinum-promoted Co15%0.1%Pt/Al<sub>2</sub>O<sub>3</sub> and Co25%0.1%Pt/Al<sub>2</sub>O<sub>3</sub> catalysts, the reaction rate increases almost linearly with cobalt content. The methane selectivity was between 7 and 20%, while the selectivity to C<sub>5+</sub> hydrocarbons was in the range from 65 to 85%. As expected, the hydrocarbon selectivities were affected by carbon monoxide conversion. Higher methane and lower C<sub>5+</sub> selectivities were observed on the cobalt catalysts at lower carbon monoxide conversion level. In agreement with previous reports [36,38–40], promotion with small amounts of platinum (0.1 wt.%) does not noticeably affect the hydrocarbon selectivity.

The catalytic performance of iron catalysts in FT synthesis is usually attributed to the presence of iron carbide species. These iron carbide species can be produced during catalyst activation and FT synthesis. Different procedures for the activation of iron FT catalysts have been subject of numerous reports. Most of them focus on the activation of bulk iron catalysts. Bukur et al. [41,42] investigated activation procedures for the 100Fe/5Cu/4.2 K/25SiO<sub>2</sub> catalyst in hydrogen, carbon monoxide and syngas. The catalyst activated in hydrogen showed higher FT reaction rate but at the same time exhibited higher methane selectivity, while the catalyst activation in carbon monoxide and syngas led to higher selectivity to long-chain hydrocarbons. These results are also consistent with recent work by Cano et al. [43]. The effect of the composition of activating gas mixture on the performance of precipitated iron catalyst was also studied by Sudsakorn [44] using SSITKA. The catalysts activated in hydrogen showed higher activity at steady state conditions. Pirola et al. [45] showed that the best catalytic performance can be obtained when the high loaded iron catalysts are activated in syngas. These results are also consistent with the report by Herranz [46]. Syngas pre-treatment yielded the most active catalysts for both unpromoted and Mn- or Ce-promoted samples. Luo

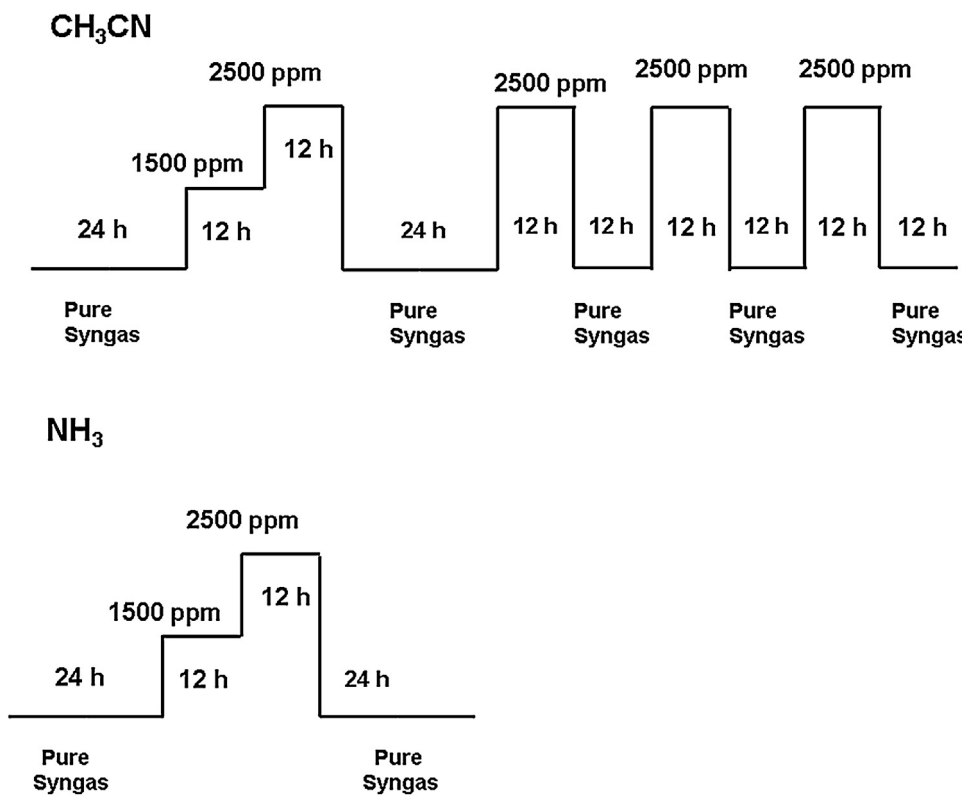


**Fig. 1.** Experimental procedures used for addition of acetonitrile and ammonia.

et al. [47,48] showed that activation of the Fe100/K1.4/Si4.6/Cu2.0 catalyst with CO produced the highest syngas conversion while activation in hydrogen generated less active catalysts. Positive effect of activation in carbon monoxide on the catalytic performance of iron catalysts in slurry reactor was also observed by O'Brien et al. [49,50], while the selectivity was not affected by the gas used for catalyst activation. It seems that the activation procedure should be adapted to specific catalysts. In the present work the catalysts were activated either in carbon monoxide or in hydrogen.

The catalytic activity of iron catalysts measured at 300 °C was strongly dependent on the support. Iron catalysts supported by carbon materials exhibited much higher FT reaction rate compared with those supported by oxides (e.g. alumina and silica). Further information about the influence of the catalytic support on the

catalytic performance of iron catalysts is available from recent publication [33]. The methane selectivity under these conditions was between 13 and 26%, while the selectivity to C<sub>5</sub>+ hydrocarbons was in the range from 13 to 31%. Note that iron catalysts exhibited very significant selectivity to carbon dioxide which increases with an increase in carbon monoxide conversion. Water is a major product of FT synthesis and high carbon dioxide selectivity observed on iron catalysts was attributed to the fast water gas shift reaction: CO + H<sub>2</sub>O ⇌ CO<sub>2</sub> + H<sub>2</sub>. Table 2 shows that carbon dioxide selectivity increases with carbon monoxide conversion. FT synthesis on iron catalysts is interplay of a large number of catalytic reactions. Depending on the rates of these reactions, the yield of carbon monoxide varies in a broad range. The maximum theoretically possible CO<sub>2</sub> selectivity is 50%.

**Table 2**

Performance of iron and cobalt catalysts at different GHSV in pure syngas before co-feeding with nitrogen containing compounds.

Catalyst	T, °C	GHSV, cm <sup>3</sup> g <sub>cat</sub> <sup>-1</sup> h <sup>-1</sup>	Catalytic performance after 24 h run					
			FT rate, 10 <sup>-7</sup> mol <sub>CO</sub> g <sub>cat</sub> <sup>-1</sup> s <sup>-1</sup>	CO conv., %	Selectivity (%)		C <sub>2</sub> –C <sub>4</sub> olefins/paraffins	
			CH <sub>4</sub>	CO <sub>2</sub>	C <sub>5</sub> <sup>+</sup>			
Cobalt catalysts	220	6750	1.9	6.8	20.7	0	64.1	3.3
		3375	2.3	16.4	11.8	0	77.8	2.1
Co15%0.1%Pt/γ-Al <sub>2</sub> O <sub>3</sub>	220	13500	5.9	10.6	19.1	0	65.9	2.2
		6750	10.1	36.2	9.3	0	81.5	1.6
Co25%0.1%Pt/γ-Al <sub>2</sub> O <sub>3</sub>	220	13500	30.2	54.1	7.5	0.3	85.9	0.9
		6750	22.0	78.7	7.3	1.0	85.1	0.8
Iron catalysts	300	16 000	27.7	39.7	21.9	33.7	13.1	0.6
		6750	25.6	91.7	13.7	38	20.5	0.7
Fe10%/SiO <sub>2</sub>	300	16 000	14.4	20.7	26.3	20.4	13.7	0.8
		6750	8.3	29.7	13.2	24.4	16.9	0.7
Fe10%/γ-Al <sub>2</sub> O <sub>3</sub>	300	6750	11.8	42.4	15.1	24.6	31.7	1.0
		16 000	30.1	43.1	19.6	30.8	16.7	1.1
		6750	21.3	76.2	15.2	37.1	17.6	0.4

### 3.3. FT synthesis with syngas containing acetonitrile and ammonia

#### 3.3.1. Influence on the FT reaction rate

FT catalytic data obtained in the presence of ammonia and acetonitrile over cobalt and iron catalysts are presented in Table 2 and Figs. 2–6. Acetonitrile is not stable at the reaction conditions in the presence of water. It undergoes hydrolysis into acetic acid and ammonia with subsequent partial decomposition of acetic acid into methane and CO<sub>2</sub>: CH<sub>3</sub>CN + 2H<sub>2</sub>O = CH<sub>3</sub>COOH + NH<sub>3</sub> = NH<sub>3</sub> + CO<sub>2</sub> + CH<sub>4</sub>. The Co based catalysts almost do not produce carbon dioxide during FT synthesis. Some slight increase in CO<sub>2</sub> on cobalt catalysts in the presence of added CH<sub>3</sub>CN may indicate partial decomposition of acetonitrile. Aqueous ammonia (30 wt.%) also has been added in order to check the main effect of acetonitrile as the source of ammonia.

The FT reaction rates measured during and after addition of different amounts of acetonitrile and ammonia to the alumina supported cobalt catalysts are given in Fig. 2. Addition of acetonitrile results in lower FT reaction rates on all studied cobalt catalysts. The activity decrease depends on the amounts of co-fed acetonitrile and on gas space velocity. Higher acetonitrile concentrations result in a more significant decrease in FT reaction rate which is due to the higher acetonitrile amounts in contact with the catalyst. Interestingly, the activity drops more rapidly during acetonitrile addition at higher syngas space velocity. Indeed, at the same reaction time and acetonitrile concentrations in the feed, the catalysts are exposed to more significant amounts of acetonitrile when the syngas space velocity is higher. After several exposures to different amounts of acetonitrile separated by the periods when the catalysts were in contact with pure syngas (Figs. 1 and 2a), all cobalt catalysts reaches a non-reversible deactivation steady state behaviour. In this quasi-steady state, the catalytic activity is not any more affected by the presence of acetonitrile in the gas feed. FT reaction rate at this state is between two and four times smaller than the initial steady state activity of the same catalysts in pure syngas. Aqueous ammonia deactivates the catalysts in the similar way, however, not so strongly in comparison with acetonitrile.

Iron catalysts show different behaviours (Fig. 3) in the presence of CH<sub>3</sub>CN and ammonia compared to cobalt catalysts. The FT reaction rate in the presence of acetonitrile and ammonia decreases for Fe10%/AC, sharply surges for Fe10%/CNT (in the case of high GHSV) and slightly increases in case of Fe10%/SiO<sub>2</sub> and Fe10%/Al<sub>2</sub>O<sub>3</sub>. The activity loss in case of 10Fe/AC can be partially recovered when co-feeding with CH<sub>3</sub>CN is stopped. At the quasi steady state obtained by periodic exposure of supported iron catalysts to acetonitrile and pure syngas (Fig. 3), the FT reaction rates is almost the same as was measured on the fresh catalysts. Addition of ammonia also produces relatively small effect on the activity of supported iron catalysts, except for Fe10%/CNT which activity dramatically increases after addition of 1500 ppm of NH<sub>3</sub> and then drops at higher NH<sub>3</sub> level.

Thus, the catalytic tests suggest different effects on added acetonitrile and ammonia on the FT reaction rates over cobalt and iron catalysts. On cobalt catalysts, acetonitrile and NH<sub>3</sub> additions result in progressive irreversible catalyst deactivation, while on iron catalysts the carbon monoxide conversion rate is affected by co-feeding with nitrogen containing compounds to a much smaller extent. Moreover, higher FT reaction rates were observed on CNT, silica and alumina supported iron catalysts in the presence of acetonitrile and ammonia.

#### 3.3.2. Effect of added acetonitrile and ammonia on the reaction selectivity

The hydrocarbon selectivities and C<sub>2</sub>–C<sub>4</sub> olefin to paraffin ratios as functions of carbon monoxide conversion on cobalt catalysts are

shown in Fig. 4. Introduction of acetonitrile and ammonia leads to lower carbon monoxide conversions (at similar GHSV) and lower FT reaction rates during and after CH<sub>3</sub>CN and NH<sub>3</sub> addition compared to pure syngas. Interestingly, the methane and C<sub>5+</sub> hydrocarbon selectivities were respectively much lower and higher at the same conversion levels on the supported cobalt catalysts during and after addition of the nitrogen containing compounds. Previously, similar effects on hydrocarbon selectivities on cobalt catalysts were observed after addition of small amounts of water [51–54] and ammonia [21] to the syngas feed. One of the possible explanations of these phenomena could be selective poisoning of cobalt methanation sites by added ammonia and its derivatives.

The olefin to paraffin ratio is also affected by co-feeding. The olefin to paraffin ratio at similar carbon monoxide conversions significantly increases. The decrease in methane selectivity is accompanied by higher olefin to paraffin ratio which could result from the lower hydrogenation activity in the presence of ammonia. Note that the effect of added acetonitrile and ammonia on the reaction selectivity was rather irreversible on cobalt catalysts. The return to pure syngas after switching off acetonitrile and ammonia cofeeding does not result in full recovering the C<sub>5+</sub> and methane selectivities to the values observed with the fresh catalyst in pure syngas (Fig. 4). Only the olefin/paraffin ratio almost comes to the same values as they were before addition of N-containing compounds.

The selectivity data plotted versus carbon monoxide conversion measured over different iron catalysts in the presence of nitrogen containing compounds are shown in Fig. 5. Exposure to different concentrations of acetonitrile results in a irreversible decrease in methane selectivities for all the supported iron catalysts. Addition of acetonitrile also affects the hydrogenation activity of iron catalysts. The olefin to paraffin ratio at similar carbon monoxide conversion increases in the presence of acetonitrile. Iron catalysts usually exhibit higher olefin selectivities compared to cobalt counterparts. In our case, the ratio of olefins to paraffins was very low (about 1) before addition of acetonitrile or ammonia (Fig. 5). This fact could be explained by different activation procedure in hydrogen in comparison with traditionally used CO activation. CO activation results in formation of iron carbide which is supposed to be an active phase in the FT synthesis over Fe catalysts. The reduction of the catalyst in hydrogen results in the formation of iron oxide and small amounts of metallic Fe. High hydrogenation activity of the catalyst activated in hydrogen can be attributed to the presence of iron metallic sites. Indeed, the iron catalysts carbided in CO show significantly lower selectivity to methane and higher selectivity to olefins (Fig. 5) with the values similar to those obtained after catalysis in the presence of acetonitrile and ammonia. It is interesting to note that addition of acetonitrile did not lead to significant changes in the catalytic performance for the iron catalysts activated in carbon monoxide, while the effect of added ammonia and acetonitrile on the reaction rate and selectivity is more significant for the catalysts activated in hydrogen.

#### 3.4. Structure and performance of the cobalt and iron catalysts exposed to nitrogen containing compounds

The catalytic results suggest that the performance of cobalt and iron catalysts in FT synthesis can be affected by co-feeding with nitrogen containing compounds. The presence of acetonitrile results in the irreversible decrease in FT reaction rate on supported cobalt catalysts and important catalyst deactivation. The hydrocarbon selectivity is also affected. At comparable conversion levels, lower methane and higher C<sub>5+</sub> hydrocarbon selectivities were detected, while the olefin to paraffin ratio becomes higher. In order to provide further insights into the modification of the active sites during and after cofeeding with ammonia, the catalysts

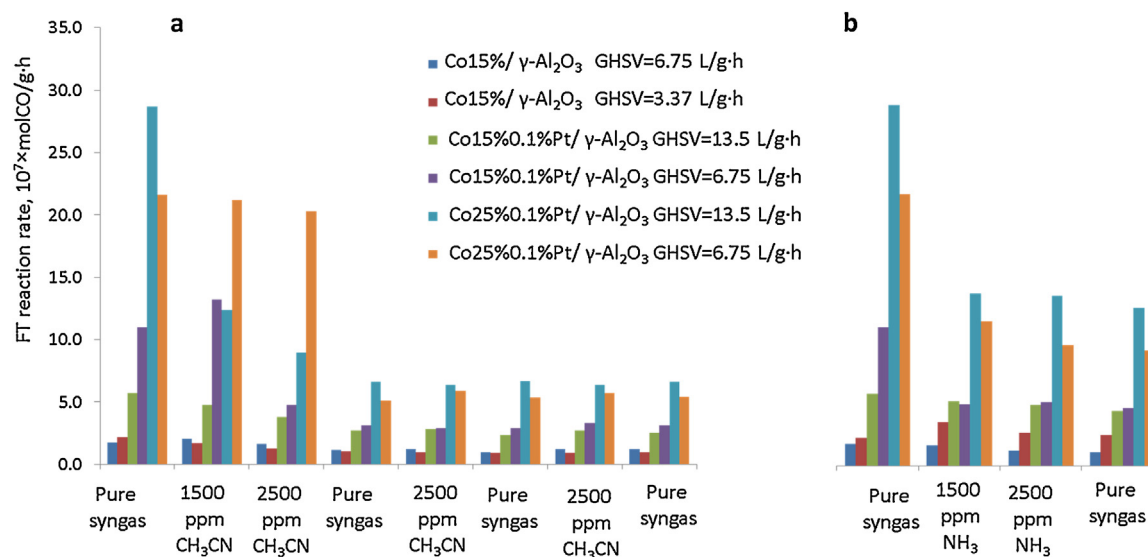


**Fig. 2.** FT reaction on cobalt catalysts measured in pure syngas and in the syngas containing different amounts of acetonitrile (a) and ammonia (b).

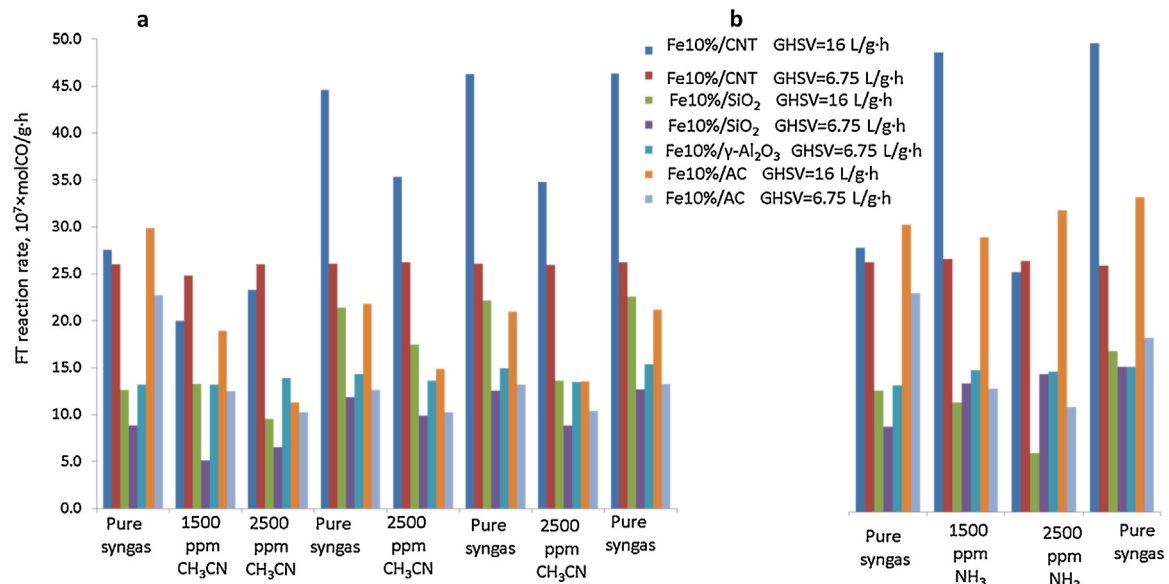


**Fig. 3.** FT reaction on iron catalysts measured in pure syngas and in the syngas containing different amounts of acetonitrile (a) and ammonia (b).

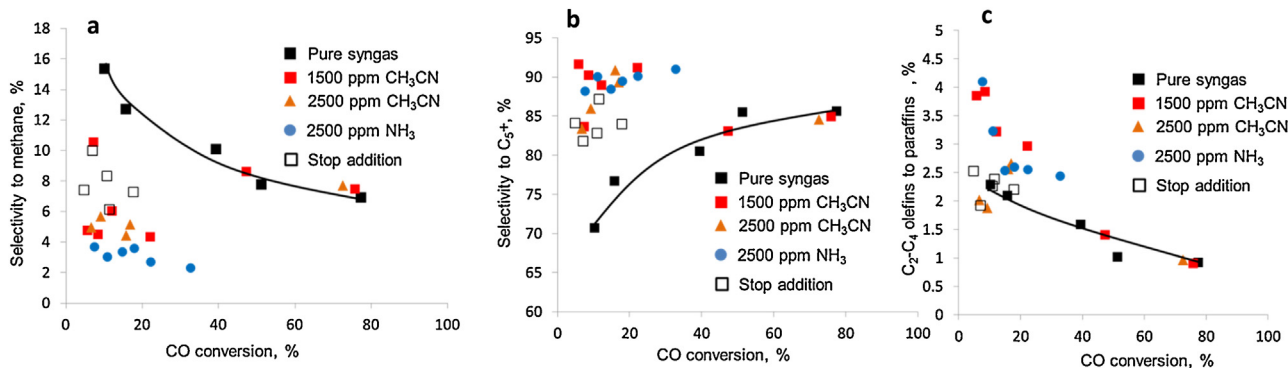


**Fig. 4.** Methane (a), C<sub>5+</sub> hydrocarbon (b) selectivities and C<sub>2</sub>-C<sub>4</sub> olefins to paraffins ratios (c) measured on supported cobalt catalysts as functions of carbon monoxide conversion in the presence of added acetonitrile and ammonia.

exposed to nitrogen-containing compounds were characterized by SSITKA with isotopic switches from <sup>12</sup>CO/H<sub>2</sub>/He/Ne to <sup>13</sup>CO/H<sub>2</sub>/He,

TPD-MS and FTIR with adsorbed carbon monoxide. The conducted catalytic tests showed low FT reaction rate on cobalt catalysts

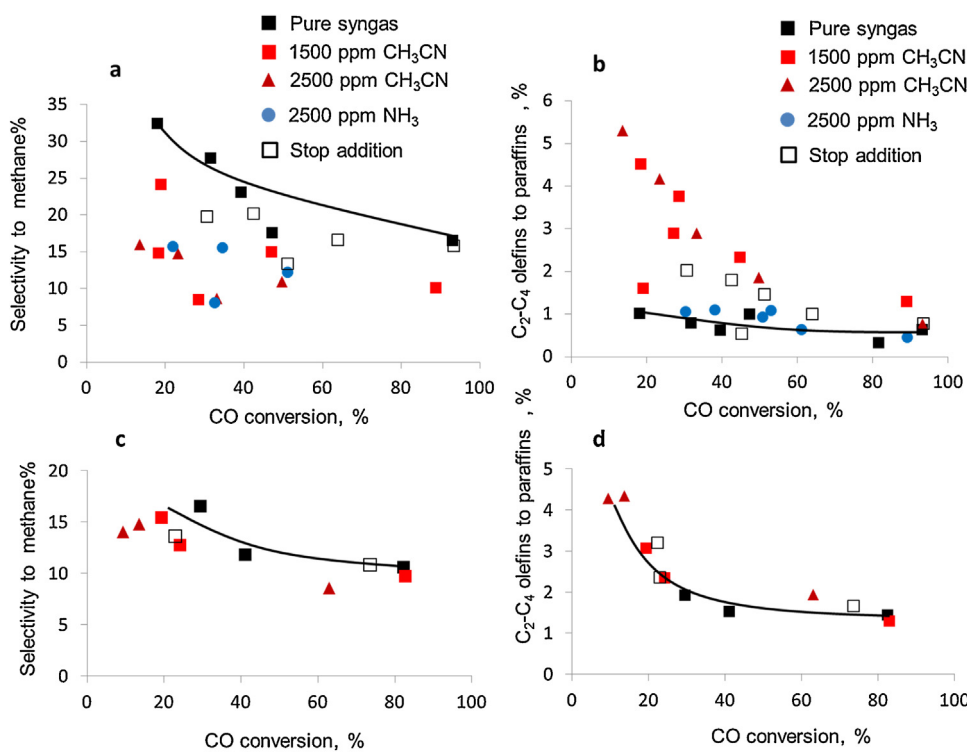


**Fig. 5.** Methane C<sub>2</sub>-C<sub>4</sub> olefins to paraffins ratios over iron catalysts activated in hydrogen (a, b) and CO (c, d) as functions of carbon monoxide conversion in the presence of acetonitrile and ammonia.

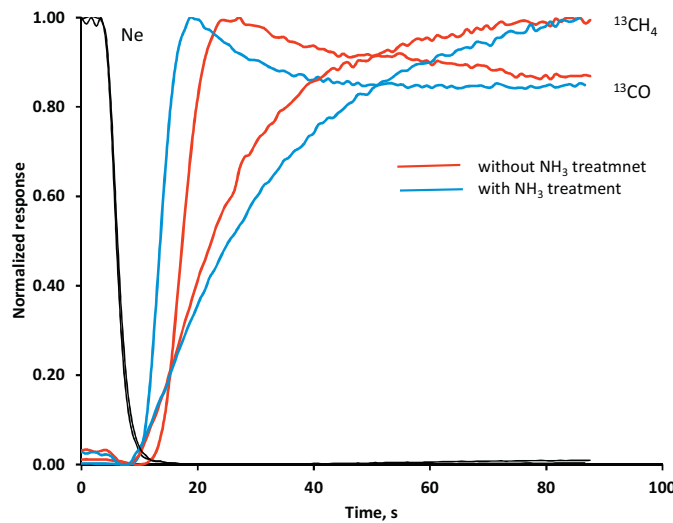


**Fig. 6.** Normalized concentrations of Ne, <sup>13</sup>CO and <sup>13</sup>CH<sub>4</sub> during switches of 12CO/H<sub>2</sub>/Ne → <sup>13</sup>CO/H<sub>2</sub> on the Co25%0.1%Pt/Al<sub>2</sub>O<sub>3</sub> catalyst without and with NH<sub>3</sub> treatment (conditions: GHSV = 14 400 cm<sup>3</sup> h<sup>-1</sup> g<sup>-1</sup>, p = 1 atm, T = 220 °C, gas composition: 5.5He:1CO:5H<sub>2</sub>:0.5Ne).

exposed to different amounts of ammonia. The decrease in reaction rate can be due to the decrease in the concentration of active sites or to the decrease in the site intrinsic activity (Turnover Frequency). Note that both phenomena can occur simultaneously during the catalyst deactivation. Unfortunately, the steady state catalytic data do not allow discriminating between these different deactivation mechanisms. SSITKA [26,55,56] addresses measuring the transient response of isotopic labels in the reactor following an abrupt change (switch) in the isotopic composition of one of the reactants. The switch involves only isotopic composition of the feed, while chemical composition remains unchanged. SSITKA provides independent

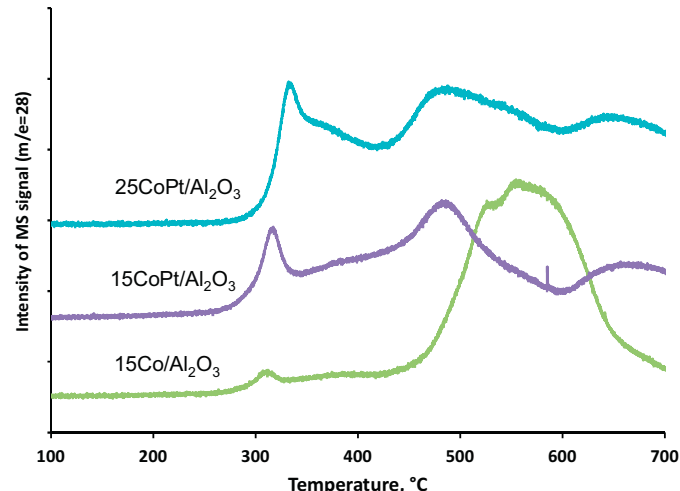


**Fig. 7.** TPD-MS profiles of alumina supported cobalt catalysts after the catalytic tests with sygas containing acetonitrile.

information about the concentration of surface intermediates and their reactivity and thus it can be extremely helpful in elucidation of the mechanism of catalyst deactivation.

The SSITKA transient curves obtained on Co25%0.1%Pt/Al<sub>2</sub>O<sub>3</sub> without and with exposure to ammonia are shown in Fig. 6. Methane was the major product of carbon monoxide hydrogenation at atmospheric pressure and using syngas with H<sub>2</sub>/CO ratio of 5. The catalyst treatment with ammonia affected transient responses of both CO and methane. The surface coverage by molecular CO and C<sub>1</sub> species and their mean surface residence time calculated from the SSITKA data are displayed in Table 3. The surface coverage by CO and its residence time are only slightly affected by ammonia treatment. At the same time, the number of C<sub>1</sub> surface intermediates has been noticeably reduced in the catalysts exposed

**Table 3**

Results of SSITKA experiments with the Co25%0.1%Pt/Al<sub>2</sub>O<sub>3</sub> catalyst without and with treatment with NH<sub>3</sub>.

Experiment	$\tau_{\text{CO}}$ (s)	$\tau_{\text{CH}_4}$ (s)	$\theta_{\text{CO}}$ ( $\mu\text{mol/g}$ )	$\theta_{\text{C}_1}$ ( $\mu\text{mol/g}$ )
Co25%0.1%Pt/Al <sub>2</sub> O <sub>3</sub> without NH <sub>3</sub> treatment	8.2	21.4	92.0	25.4
Co(25%)Pt/Al <sub>2</sub> O <sub>3</sub> with NH <sub>3</sub> treatment	8.6	29.2	105	18.8

to ammonia. The NH<sub>3</sub> treatment also notably increases the residence time of C<sub>1</sub> surface intermediates from 21.4 to 29.2 s. This suggests that ammonia treatment produces strong impact on the both concentration and reactivity of C<sub>1</sub> surface intermediates. It can be also suggested that the most active surface sites responsible for hydrogenation of adsorbed carbon species have been deactivated during the ammonia treatment. This could possibly explain lower methane selectivity on the cobalt catalysts exposed to acetonitrile and ammonia.

Thus, ammonia co-fed to the catalyst can affect the number and intrinsic activity of active sites for FT synthesis. These modifications can be possibly attributed to the formation of cobalt nitride in the presence of ammonia. In order to further confirm formation of cobalt nitride, the catalysts after exposure to ammonia during the catalytic tests were characterized by TPD-MS. Fig. 7 shows the TPD-MS profiles of the alumina supported catalysts after the catalytic tests with detection of m/e = 28. The TPD-MS profiles of all the spent catalysts exhibited sharp peaks at 300 °C measured using both m/e = 28 and m/e = 14 signals. It can be suggested that these sharp peaks observed at 300 °C correspond to desorption of nitrogen. This nitrogen can be produced from cobalt nitride decomposition. The amount of nitrogen calculated from the area of this peak correlates with the amount of reduced cobalt in the catalysts: the N/Co ratios were 0.46 for Co15%/Al<sub>2</sub>O<sub>3</sub>, 0.74 for Co15%0.1%Pt/Al<sub>2</sub>O<sub>3</sub> and 0.73 for Co25%0.1%Pt/Al<sub>2</sub>O<sub>3</sub>. Cobalt nitride formation in the presence of ammonia has been reported in previous works [57–59]. The catalytic results obtained in this work suggest that cobalt nitride is not active in FT synthesis. Indeed, formation of cobalt nitride during the catalyst exposure to acetonitrile leads to important catalyst deactivation. At the same time, cobalt nitride formation coincides with the modifications of FT catalyst selectivity patterns and leads to lower methane and higher C<sub>5+</sub>

hydrocarbon selectivities. This suggests that the cobalt nitride formation proceeds selectively on the sites favouring methanation and block the most active cobalt hydrogenating sites.

Fig. 8 shows the IR spectra of carbon monoxide adsorbed on the Co15%/Al<sub>2</sub>O<sub>3</sub> and Co15%0.1%Pt/Al<sub>2</sub>O<sub>3</sub> catalysts activated in hydrogen and then pre-treated with ammonia. The spectra exhibit a set of bands of adsorbed carbon monoxide. The broad band with the frequency from 2000 to 2100 cm<sup>-1</sup> can be assigned to CO adsorption on cobalt sites, while the bands at 2179 and 2159 cm<sup>-1</sup> seem to be attributed to CO adsorption on Lewis acid sites and hydroxyl groups of the alumina support, respectively. Catalyst exposure to ammonia results in the modification of the shape of the broad low frequency CO band. In particular, the broad band gets narrower and contribution of the lower frequencies ( $\nu_{\text{CO}} = 2029 \text{ cm}^{-1}$ ) branch is slightly reduced. This fact suggests that ammonia pre-treatment results in disappearance of electron enriched cobalt surface sites, associated with low-frequency shoulder. Previous reports [60–62] attribute low frequency bands with the frequency of 2000–2030 cm<sup>-1</sup> to the CO molecules in interaction with the edges or step sites of metal nanoparticles (Pt or Pd), while the band of CO with high frequencies ( $\nu_{\text{CO}} = 2040–2060 \text{ cm}^{-1}$ ) corresponds to the adsorption on the terraces. It could be speculated therefore that cobalt nitride species could preferentially form on these highly unsaturated metal sites (Fig. 9). The blockages of edges and steps of cobalt metal nanoparticles by nitrides could result in the decrease in the FT reaction rates and modify the reaction selectivity. Addition of platinum to the catalyst (Fig. 8b) promotes this process and decreases the amount of unsaturated Co sites. Initially higher amount of active sites (bands at 2029 cm<sup>-1</sup> in Fig. 8a and b) leads to higher activity of Pt-promoted catalyst in comparison with unpromoted catalyst.

Differently to supported cobalt catalysts, the exposure of supported iron catalysts to acetonitrile and ammonia does not lead

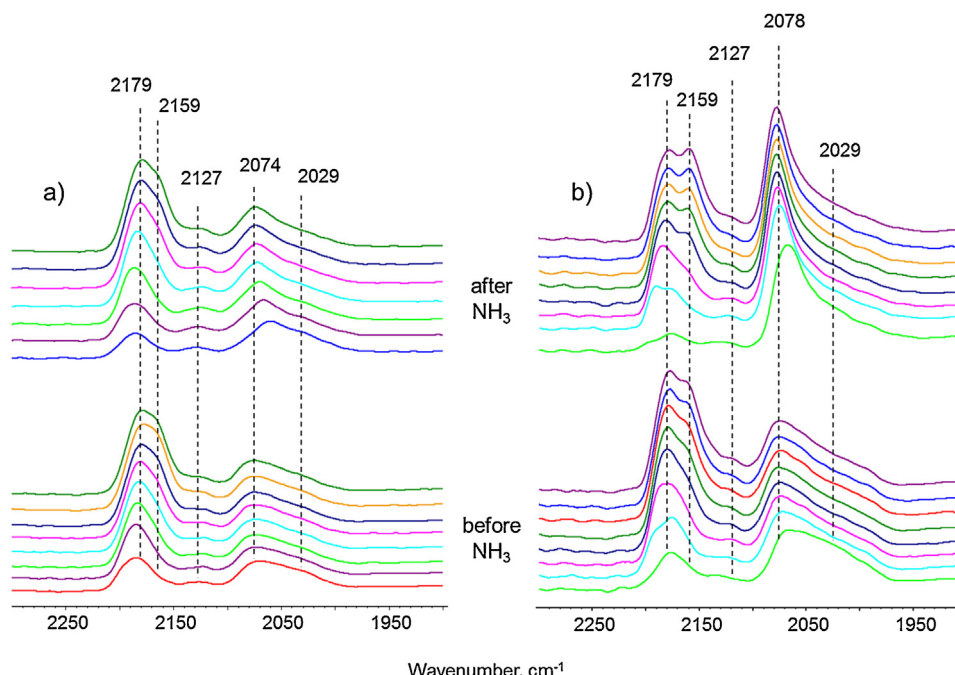
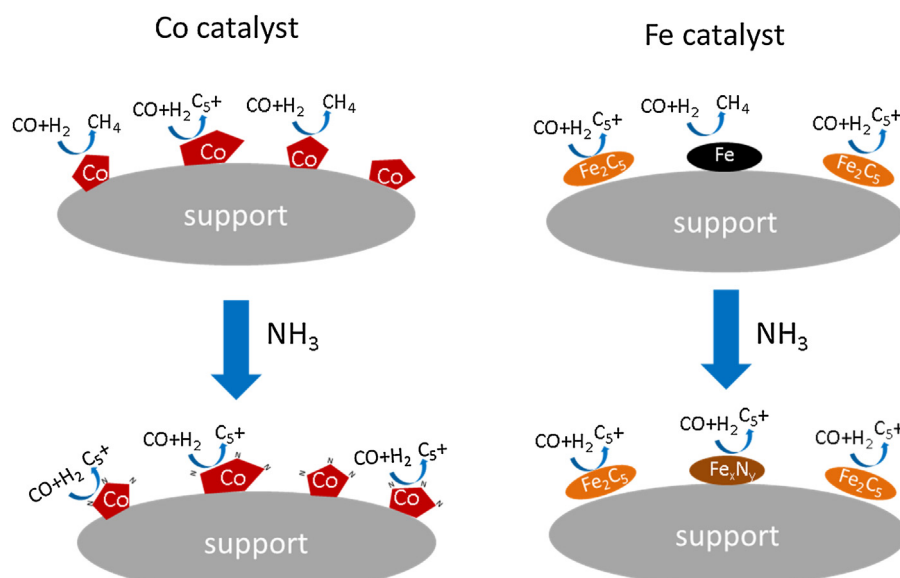


Fig. 8. FTIR spectra of carbon monoxide adsorbed on the activated Co15%/Al<sub>2</sub>O<sub>3</sub> (a) and Co25%0.1%Pt/Al<sub>2</sub>O<sub>3</sub> (b) catalysts before and after exposure to NH<sub>3</sub>.



**Fig. 9.** Evolution of cobalt and iron catalysts in the presence of ammonia.

to any irreversible catalyst deactivation. Interaction of the ammonia with the iron catalysts under the reaction conditions can result in formation of iron nitrides. The catalytic activity of iron nitrides in FT synthesis have been investigated since the pioneering works of Anderson [63,64]. The activity of iron nitride is comparable of that of iron carbides, though the two phases exhibit some differences relevant to the reaction selectivity [63–65]. Shultz et al. [64] also showed that the iron nitride could be converted rapidly into iron carbo-nitrides if the ammonia has not been fed any more to the reactor. Upon further treatment with syngas, the carbo-nitride changed to Hägg carbide, which is usually considered as an active phase for FT synthesis over iron catalysts [3,12,13]. Iron carbides after the FT reaction tests in our spent iron catalysts were previously detected [33] using XRD and Mossbauer spectrometry. The present work is indicative of very small effect of acetonitrile on their catalytic performance of iron catalysts activated in CO, while significant modifications of the hydrogenation activity in the case of the iron catalyst activated in hydrogen were observed. High hydrogenation activity was attributed to the presence of metallic iron in the catalysts activated in hydrogen. Ammonia addition seems to facilitate conversion of iron oxides and metallic iron in the catalysts activated in hydrogen into iron nitride and then to iron carbide in the presence of syngas (Fig. 9). Catalytic properties of different iron phases present under the reaction conditions in pure syngas (iron carbide) and in the presence of acetonitrile (iron carbide, iron nitride or iron carbo-nitride) could probably explain a relative stability of FT reaction rate in the presence of small concentrations of acetonitrile in syngas over iron catalysts.

#### 4. Conclusion

The catalytic performance of supported cobalt and iron catalysts in respectively low and high temperature FT synthesis is affected in a different manner by the presence of small amounts of acetonitrile and ammonia in the syngas feed. Acetonitrile and ammonia addition during FT synthesis to supported cobalt catalysts results in irreversible catalyst deactivation which is probably due to the formation of inactive cobalt nitride. Cobalt nitride possibly forms on the steps and edges of cobalt nanoparticles and selectively blocks the sites responsible for methanation. The intrinsic hydrogenation activity of cobalt sites decreases after cobalt nitride formation.

Consequently lower methane and higher C<sub>5+</sub> hydrocarbon selectivities were observed on cobalt catalysts exposed to acetonitrile and ammonia.

No noticeable deactivation was observed on the exposure of supported iron catalysts to acetonitrile and ammonia. The effect of nitrogen-containing additives on iron catalysts depends on the activation procedure. Catalyst activation in hydrogen results in irreversible modifications of the catalyst selectivity patterns after ammonia addition. The methane selectivity is reduced, while the olefins to paraffins ratio is increased. Iron catalysts activated in carbon monoxide did not demonstrate any effect of acetonitrile addition on the selectivity.

#### Acknowledgments

The authors gratefully acknowledge financial support for this work from the French National Agency for Research (Biosyngop Project, Ref. ANR- 11-BS07-026). The authors are indebted to S. Heyte and J. Thuriot for technical assistance with high throughput catalytic experiments. The REALCAT platform is benefiting from a Governmental subvention administrated by the French National Research Agency (ANR) within the frame of the 'Future Investments' program (PIA), with the contractual reference 'ANR-11-EQPX-0037'. The Nord-Pas-de-Calais Region and the FEDER are acknowledged for their financial contribution to the acquisition of the equipment of the platform. A.C. is grateful to CAPES-COFECUB program (Brazil-France) for supporting his Ph.D. research.

#### References

- [1] R.L. Espinoza, A.P. Steynberg, B. Jager, A.C. Vosloo, *Appl. Catal. A* 186 (1999) 13–26.
- [2] A.Y. Khodakov, *Catal. Today* 144 (2009) 251–257.
- [3] A.P. Steynberg, R.L. Espinoza, B. Jager, A.C. Vosloo, *Appl. Catal. A* 186 (1999) 41–54.
- [4] N.E. Tsakoumis, M. Rønning, Ø. Borg, E. Rytter, A. Holmen, *Catal. Today* 154 (2010) 162–182.
- [5] A.M. Saib, D.J. Moodley, I.M. Ciobăcă, M.M. Hauman, B.H. Sigwela, C.J. Weststrate, J.W. Niemantsverdriet, J. van de Loosdrecht, *Catal. Today* 154 (2010) 271–282.
- [6] M. Asadullah, *Renew. Sustain. Energy Rev.* 40 (2014) 118–132.
- [7] A.H. Lillebø, A. Holmen, B.C. Enger, E.A. Blekkan, *WIREs Energy Environ.* 2 (2013) 508–524.
- [8] E. van Steen, M. Claeys, *Chem. Eng. Technol.* 31 (2008) 655–666.

- [9] K. Kim, Y. Kim, C. Yang, J. Moon, B. Kim, J. Lee, U. Lee, S. Lee, J. Kim, W. Eom, S. Lee, M. Kang, Y. Lee, M. Kang, Y. Lee, Biore sour. Technol. 127 (2013) 391–399.
- [10] M. Ehrensperger, J. Winterlin, J. Catal. 329 (2015) 49–56.
- [11] A.S. Bambal, V.S. Guggilla, E.I. Kugler, T.H. Gardner, D.B. Dadyburjor, Ind. Eng. Chem. Res. 53 (2014) 5846–5857.
- [12] H.M. Torres Galvis, A.C.J. Koeken, J.H. Bitter, T. Davidian, M. Ruitenbeek, A.I. Dugulan, K.P. de Jong, Catal. Today 215 (2013) 95–102.
- [13] D.E. Sparks, G. Jacobs, M.K. Gnanamani, V.R.R. Pendyala, W. Ma, J. Kang, W.D. Shafer, R.A. Keogh, U.M. Graham, P. Gao, B.H. Davis, Catal. Today 215 (2013) 67–72.
- [14] H.M. Torres Galvis, A.C.J. Koeken, J.H. Bitter, T. Davidian, M. Ruitenbeek, A.I. Dugulan, K.P. de Jong, J. Catal. 303 (2013) 22–30.
- [15] Ø. Borg, N. Hammer, B.C. Enger, R. Myrstad, O.A. Lindvåg, S. Eri, T.H. Skagseth, E. Rytter, J. Catal. 279 (2011) 163–173.
- [16] S.S. Pansare, A.J. Allison, Appl. Catal. A 387 (2010) 224–230.
- [17] C.G. Visconti, L. Lietti, E. Tronconi, P. Forzatti, R. Zennaro, S. Rossinic, Catal. Today 154 (2010) 202–209.
- [18] N. Koizumi, K. Murai, T. Ozaki, M. Yamada, Catal. Today 89 (2004) 465–478.
- [19] H.J. Robotra, J. Alger, P.J. Pretorius, 12AIChE—2012 AIChE Spring Meeting and 8th Global Congress on Process Safety, Conference Proceedings (2012), 1p.
- [20] S.C. LeVinnies, C.J. Mart, W.C. Behrmann, S.J. Hsia, D.R. Neskorra, WO Patent 050487 (1998) assigned to Exxon research and engineering company.
- [21] V.R.R. Pendyala, M.K. Gnanamani, G. Jacobs, W. Ma, W.D. Shafer, B.H. Davis, Appl. Catal. A 468 (2013) 38–43.
- [22] W. Ma, G. Jacobs, D.E. Sparks, V.R.R. Pendyala, S.G. Hopps, G.A. Thomas, H.H. Hamdeh, A. MacLennan, Y. Hu, B.H. Davis, J. Catal. 326 (2015) 149–160.
- [23] T. Sango, N. Fischer, R. Henkel, F. Roessner, E. van Steen, M. Claeys, Appl. Catal. A 502 (2015) 150–156.
- [24] <http://avantium.com/uploads/brochures/avantium-chemicals-flowrence.pdf>.
- [25] P. Scherrer, Göttinger Nachrichten, R. Zsigmondy, Kolloidchemie (3rd Ed. 1920), (1918) p. 394.
- [26] B. Legras, V.V. Ordomsky, C. Dujardin, M. Virginie, A.Y. Khodakov, ACS Catal. 4 (2014) 2785–2791.
- [27] M. Sadeqzadeh, H. Karaca, O.V. Safanova, P. Fongarland, S. Chambrey, P. Roussel, A. Griboval-Constant, M. Lacroix, D. Curulla-Ferré, F. Luck, A.Y. Khodakov, Catal. Today 164 (2011) 62–67.
- [28] H. Karaca, O.V. Safanova, S. Chambrey, P. Fongarland, P. Roussel, A. Griboval-Constant, M. Lacroix, A.Y. Khodakov, J. Catal. 277 (2011) 14–26.
- [29] A. Jean-Marie, A. Griboval-Constant, A.Y. Khodakov, F. Diehl, CR Chim. 12 (2009) 660–667.
- [30] D. Peña, A. Griboval-Constant, C. Lancelot, M. Quijada, N. Visez, O. Stéphan, V. Lecocq, F. Diehl, A.Y. Khodakov, Catal. Today 228 (2014) 65–76.
- [31] D. Peña, A. Griboval-Constant, V. Lecocq, F. Diehl, A.Y. Khodakov, Catal. Today 215 (2013) 43–51.
- [32] A. Griboval-Constant, A. Butel, V.V. Ordomsky, P.A. Chernavskii, A.Y. Khodakov, Appl. Catal. A 481 (2014) 116–126.
- [33] K. Cheng, V.V. Ordomsky, M. Virginie, B. Legras, P.A. Chernavskii, V.O. Kazak, C. Cordier, S. Paul, Ye Wang, A.Y. Khodakov, Appl. Catal. A 488 (2014) 66–77.
- [34] K. Cheng, M. Virginie, V.V. Ordomsky, C. Cordier, P.A. Chernavskii, M.I. Ivantsov, S. Paul, Y. Wang, A.Y. Khodakov, J. Catal. 328 (2015) 139–150.
- [35] D. Schanke, S. Vada, E.A. Blekkan, A.M. Hilmen, A. Hoff, A. Holmen, J. Catal. 156 (1995) 85–95.
- [36] F. Diehl, A.Y. Khodakov, Oil Gas Sci. Technol. 64 (2009) 11–24.
- [37] W. Chu, P.A. Chernavskii, L. Gengembre, G.A. Pankina, P. Fongarland, A.Y. Khodakov, J. Catal. 252 (2007) 215–230.
- [38] S. Vada, A. Hoff, E. Ådnane, D. Schanke, A. Holmen, Top. Catal. 2 (1995) 155–162.
- [39] H. Zhang, W. Chu, C. Zou, Z. Huang, Z. Ye, L. Zhu, Catal. Lett. 141 (2011) 438–444.
- [40] A.Y. Khodakov, W. Chu, P. Fongarland, Chem. Rev. 107 (2007) 1692–1744.
- [41] D.B. Bukur, L. Nowicki, R.K. Manne, X. Lang, J. Catal. 155 (1995) 366–375.
- [42] D.B. Bukur, L. Nowicki, X. Lang, Catal. Today 24 (1995) 111–119.
- [43] L.A. Cano, M.V. Cagnoli, J.F. Bengoa, A.M. Alvarez, S.G. Marchetti, J. Catal. 278 (2011) 310–320.
- [44] K. Sudsakorn, J.G. Goodwin Jr., A.A. Adeyiga, J. Catal. 213 (2003) 204–210.
- [45] C.C. Pirola, L. Bianchi, A. Di Michele, P. Diodati, S. Vitali, V. Ragaini, Catal. Lett. 131 (2009) 294–304.
- [46] T. Herranz, S. Rojas, F.J. Pérez-Alonso, M. Ojeda, P. Terreros, J.L.G. Fierro, J. Catal. 243 (2006) 199–211.
- [47] M. Luo, B.H. Davis, Fuel Process. Technol. 83 (2003) 49–56.
- [48] M. Luo, H. Hamdeh, B.H. Davis, Catal. Today 140 (2009) 127–134.
- [49] R.J. O'Brien, L. Xu, R.L. Spicer, S. Bao, D.R. Milburn, B.H. Davis, Catal. Today 36 (1997) 325–334.
- [50] R.J. O'Brien, L. Xu, R.L. Spicer, B.H. Davis, Energy Fuels 10 (1996) 921–926.
- [51] Ø. Borg, S. Storsæter, S. Eri, H. Wigum, E. Rytter, A. Holmen, Catal. Lett. 107 (2006) 95–102.
- [52] S. Storsæter, Ø. Borg, E.A. Blekkan, A. Holmen, J. Catal. 231 (2005) 405–419.
- [53] A.K. Dalai, B.H. Davis, Appl. Catal. A 348 (2008) 1–15.
- [54] W. Ma, G. Jacobs, T.K. Das, C.M. Masuku, J. Kang, V.R.R. Pendyala, B.H. Davis, J.L.S. Klettlinger, C.H. Yen, Ind. Eng. Chem. Res. 53 (2014) 2157–2166.
- [55] S.L. Shannon, J.G. Goodwin, Chem. Rev. 95 (1995) 677–695.
- [56] A.M. Efstatthiou, J.T. Gleaves, G.S. Yablonsky, Characterisation of Solid Materials: From Structure to Surface Reactivity, in: M. Che, J.C. Vedrine (Eds.), Ch. 22 – Transient Techniques: Temporary Analysis of Products (TAP) and Steady State Isotopic Transient Kinetic Analysis (SSITKA), Wiley VCH, 2012, pp. 1013–1073.
- [57] Z. Yao, A. Zhu, J. Chen, X. Wang, C.T. Au, C. Shi, J. Solid State Chem. 180 (2007) 2635–2640.
- [58] R. Marchand, F. Tessier, F.J. DiSalvo, J. Mater. Chem. 9 (1999) 297–304.
- [59] Y. Shi, Y. Wan, R. Zhang, D. Zhao, Adv. Funct. Mater. 18 (2008) 2436–2443.
- [60] K. Wolter, O. Seiferth, J. Libuda, H. Kuhlenbeck, M. Bäumer, H.-J. Freund, Surf. Sci. 402–404 (1998) 428–432.
- [61] K. Kunimatsu, T. Sato, H. Uchida, M. Watanabe, Electrochim. Acta 53 (2008) 6104–6110.
- [62] D.R. Rainer, M.-C. Wu, D.I. Mahon, D.W. Goodman, J. Vac. Sci. Technol. A 14 (1996) 1184–1188.
- [63] R.B. Anderson, J.F. Shultz, B. Seligman, W.K. Hall, H.H. Storch, J. Am. Chem. Soc. 72 (1950) 3502–3508.
- [64] J.F. Shultz, B. Seligman, J. Lecky, R.B. Anderson, J. Am. Chem. Soc. 74 (1952) 637–640.
- [65] E.B. Yeh, L.H. Schwartz, J.B. Butt, J. Catal. 91 (1985) 241–253.